Radial Segregation Patterns in Rotating Granular Mixtures: Waviness Selection

K. M. Hill, G. Gioia, and D. Amaravadi

Department of Theoretical and Applied Mechanics, University of Illinois, Urbana, Illinois 61801, USA

(Received 22 December 2003; revised manuscript received 26 August 2004; published 22 November 2004)

We model the radial segregation patterns that form in a thin rotating drum partially filled with beads of two sizes. We predict that the waviness (or amplitude-to-wavelength ratio, denoted w) of a pattern should be subjected to low-pass filtering with a cutoff waviness w_c that depends strongly on the fill level of the drum. Then we perform experiments and find that $w \leq w_c$ for all patterns, in accord with our prediction. We also find that $w = w_c$ for (and only for) steady patterns, and conclude that the waviness of a steady pattern is selected by the low-pass filtering.

DOI: 10.1103/PhysRevLett.93.224301 PACS numbers: 45.70.Qj, 45.70.Mg, 47.54.+r, 89.75.Fb

When a granular mixture is vibrated or made to flow, it segregates by the type of grain [1]. For instance, if a bed of grains of different sizes is sheared parallel to the top surface, the larger grains segregate to the surface of the bed and the smaller ones to the bottom [2]. In Nature, this form of granular segregation might explain why the gravelly bed of a piedmont stream is frequently topped with a self-organized, stabilizing *armour layer* composed of the largest rocks in the bed [3]. Granular segregation also occurs in numerous industrial processes, often with undesirable effects [4]. To study granular segregation, some researchers have used a thin rotating drum partially filled with beads of different sizes. Within the first rotation of the drum, a radial segregation pattern forms [Fig. 1(a)–1(c)] [5]. The pattern of Fig. 1(c) forms for all fill levels of the drum; we call it a *moon pattern* because it reminds us of an ashy moon on a dark sky. For most fill levels, the moon pattern appears to be steady [6]. Yet *for fill levels close to 1/2* the moon pattern evolves through a series of transient, increasingly *wavy*, striped segregation patterns or *sun patterns* as the rotation continues [Figs. 1(d)–1(g)] [7]. Upon attaining a value that depends strongly on the fill level, the *waviness* ceases to increase, and a sun pattern of the selected waviness remains steady thereafter [Fig. 1(h)] [6,7]. Here we develop a model of waviness selection in sun patterns. In developing our model, we are led to identify the waviness of a sun pattern (as yet a loose visual descriptor) with the amplitude-to-wavelength ratio of its stripes. We find that in contrast to many systems in which a wavelength is selected at the onset of a runaway process (often embodied by an eigenproblem), in sun patterns the waviness is selected when a low-pass filter arrests a runaway process of waviness amplification. To test our findings, we perform experiments and compare the results with the predictions of the model.

In our experiments we use an acrylic drum (of radius $R = 15$ cm and thickness 8 mm) filled with water [8] and, up to a distance $R + d$ measured from the bottom of the drum, with a mixture of glass beads (Jaygo Inc., NJ; $\rho = 2.54$ g/cm^3) [Fig. 2(a)]. The average composition of the mixture is 40% 3 mm black beads and 60% 1 mm white beads, by volume (measured by weight). We rotate the drum about its axis with an angular velocity $\Omega = 1$ rpm and take pictures at regular intervals (e.g., Fig. 1). By processing these pictures [9], we obtain an index of the waviness, p^2/A, where p is the perimeter of the segregation pattern and A is the area contained within the perimeter. Figure 2(b) shows a plot of p^2/A vs the number of rotations for a fill level close to $1/2$; within a few tens of rotations, p^2/A attains a steady value that depends strongly on the fill level [Fig. 2(c)].

To shed light on these results, we start by describing how the beads move in the rotating drum. The beads move relative to one another only in a shallow surficial layer of maximum depth b known as the *flowing layer* [Fig. 3(a)] [10]. Below the flowing layer the beads—and, with the beads, the segregation pattern—move in solidlike rotation with the drum. The flowing layer exchanges beads with the stratum below through the arc PMQ of Fig. 3(a). The beads positioned along the arc PM can be said to be *thawing* as they enter the flowing layer and cease to move in solidlike rotation with the drum. Thus we call PM the *thawing arc* and the flux of beads that enters the flowing

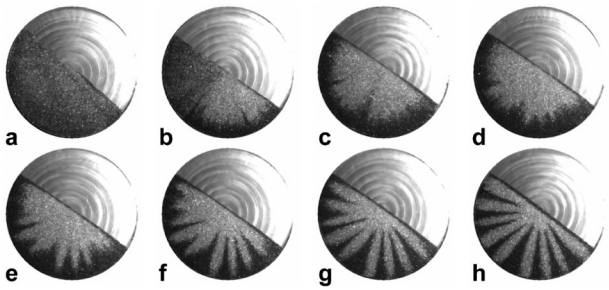

FIG. 1. (a) The drum partially filled with well mixed black and white beads. The drum after (b) 1/4 rotation, (c) 1/2 rotation (moon pattern), (d) one rotation, (e) two rotations, (f) three rotations, (g) four rotations, and (h) many rotations (steady sun pattern). In these experiments the free surface remains flat and steady as the drum rotates.

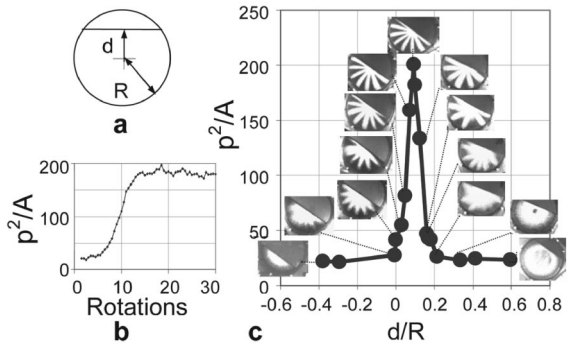

FIG. 2. (a) The drum filled to a distance $R + d$ measured from the bottom of the drum. The ratio $-1 \leq d/R \leq 1$ characterizes the fill level of the drum; if $d/R = 0$ the fill level is 1/2. (b) p^2/A vs the number of rotations of the drum for a fill level close to 1/2. (c) The steady value of p^2/A vs d/R for a range of fill levels. The steady value of p^2/A peaks for a fill level slightly higher than 1/2 ($d/R = 0.1$). For a moon pattern at a fill level of 1/2, $p^2/A = 2(2 + \pi)^2/\pi \approx 17$.

layer through PM the *thawing flux*. Likewise, we call MQ the *freezing arc* and the flux of beads that leaves the flowing layer through MQ the *freezing flux*. Consider now the experiment of Figs. 1(a)–1(c). Since the black and the white beads are initially well mixed, they enter the flowing layer in a thawing flux of constant composition (i.e., a thawing flux whose average composition is constant in time). As they move in the flowing layer the larger (black) beads segregate to the upper part of the layer, and the smaller beads to the lower part. When these beads leave the flowing layer, they begin to form a moon pattern [Fig. 3(b)]; when they reenter the flowing layer (again in a thawing flux of constant composition), the moon pattern becomes complete [Figs. 3(c) and 3(d)]. This argument [5] explains the formation of moon patterns for all fill levels. For future reference, we stress that *a thawing flux of constant composition leads to the rapid formation of a moon pattern*.

Before turning to the sun patterns, we simplify the geometry of the thawing and freezing arcs. We substitute the thawing arc PM with the straight thawing line LM and the freezing arc MQ with the straight freezing line MR [Fig. 4(a)]. The thawing and freezing lines are parallel to the free surface at a distance $|d'|$ from the axis of the drum, where $d' = d - b$. The beads positioned along the freezing line MR at a given time remain on a straight line while they rotate with the drum [Figs. 4(b) and 4(c)].

Consider now the idealized sun pattern of Fig. 4(d). For a time interval $T/2$, the beads that leave the flowing layer

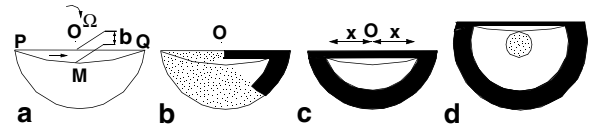

FIG. 3. (a) The flowing layer of maximum depth b is bounded by the free surface PQ and by the arc PMQ. The point O represents the axis of the drum. (b) A partially formed moon pattern. (c) A moon pattern. The value of x depends on the fill level, the average composition of the mixture, and b. (d) If $d > b$, the moon pattern includes a circle (with center at the axis of the drum) containing mixed beads that never enter the flowing layer; cf. the pictures of Fig. 2(c).

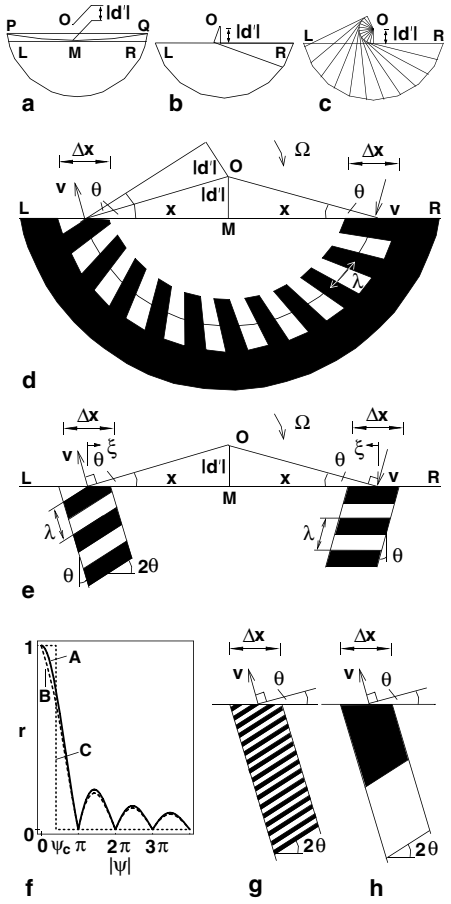

FIG. 4. (a) LM is the thawing line, MR is the freezing line. Here M is below the axis of the drum ($d' < 0$). Beads that freeze at the same time remain on a straight line (b) as they rotate with the drum (c). (d) Idealized sun pattern. The value of x pertains to the moon pattern [Fig. 3(c)]. This figure shows the sequence in which the beads leave and reenter the flowing layer for $d' < 0$. If we turn the page upside down, this same figure will show the sequence in which the beads leave and reenter the flowing layer for $d' > 0$ (but with the thawing line on the right and the freezing line on the left). Because the geometry is the same regardless of the sign of d', the equations that we derive based on this geometry apply to all fill levels. (e) A bead that freezes at a distance x–ξ to the right of M thaws at distance x–ξ to the left of M. Suppose that two beads freeze simultaneously, the 1st at $\xi = 0$ and the 2nd at $\xi = \xi'$; if the 1st thaws at a time t, the 2nd thaws at a time $t - \tau(\xi')$, where $\tau(\xi) = 2\xi \sin\theta/v$. (f) Plots of r vs $|\psi|$ for c_f equal to one term (curve A) and 20 terms (curve B) of the Fourier expansion of $S_T(t)$. Curve C is an idealization of B. A high w gives a thawing flux of constant composition (g), and a low w a thawing flux of oscillating composition (h).

through the segment Δx of the freezing line are black; then, for a time interval $T/2$, these beads are white, and so on in a cyclic fashion. Thus the beads leave the flowing layer in a freezing flux of oscillating composition. The stripes unfold in the fanlike arrangement of Fig. 4(c); they have an amplitude Δx and a wavelength $\lambda = vT$, where $v = \Omega x \sec\theta$ [Fig. 4(d)]. Figure 4(e) illustrates the sequence in which the beads of Fig. 4(d) leave (and later reenter) the flowing layer.

With the help of Fig. 4(e), we seek a mathematical characterization of the thawing and freezing fluxes. We start by defining the local composition $-1 \le c \le 1$ of a mixture in the form $c = f_b - f_w$, where f_b and f_w is the local volume fraction of black and white beads, respectively. On the freezing (or thawing) line, the local composition c may be a function of the position ξ and the time t, $c = c(\xi, t)$. [For the idealized sun pattern of Fig. 4, on the freezing line $c = c_f(\xi, t) = S_T(t)$, where $S_T(t)$ is an oscillating square function of amplitude 2 and period T, and on the thawing line $c = c_t(\xi, t) = S_T(t - \tau(\xi))$, where $\tau(\xi) = 2\xi \sin\theta/v$ is a time shift; see the caption to Fig. 4(e)]. The flux of c advected through the segment Δx of the freezing (or thawing) line is $\varphi(t) = v_n \int_{-\Delta x/2}^{\Delta x/2} c(\xi, t) d\xi$, where $v_n = \Omega x$ is the component of v normal to the freezing (or thawing) line [11]. The mean value of $\varphi(t)$, $\langle\varphi\rangle = (1/T) \int_0^T \varphi(t) dt$, is zero, because in the idealized sun pattern the white stripes have the same volume as the black stripes [12]. On the other hand, the root mean square of $\varphi(t)$, $\sqrt{\langle\varphi^2\rangle} = \sqrt{(1/T) \int_0^T \varphi^2(t) dt}$, is zero for a flux of constant composition, but positive for a flux of oscillating composition, and provides a measure of the amplitude of the compositional oscillations of the flux $\varphi(t)$. Thus, if $\varphi_f(t)$ is the freezing flux and $\varphi_t(t)$ is the thawing flux, $r = \sqrt{\langle\varphi_t^2\rangle/\langle\varphi_f^2\rangle}$ measures the extent to which the compositional oscillations of the freezing flux carry over to the thawing flux. (For example, $r < 1$ indicates that the fluxes becomes less oscillating with each freezing-and-thawing cycle.) To compute r, we take $c_f(\xi, t) = 4\cos(2\pi t/T)/\pi$ [the first term in the Fourier expansion of $S_T(t)$], and therefore $c_t(\xi, t) = 4\cos[2\pi(t - \tau(\xi))/T]/\pi$, where $\tau(\xi) = 2\xi \sin\theta/v$. The result is $r = \sin|\psi|/|\psi|$, where $\psi = 2\pi w \sin\theta$ and $w = \Delta x/\lambda$, i.e., the amplitude-to-wavelength ratio or *waviness*. Curve A in Fig. 4(f) is a plot of r vs $|\psi|$. We have also computed r by taking c_f equal to the first 20 terms in the Fourier expansion of $S_T(t)$, with a similar result [curve B in Fig. 4(f)]. In both curves A and B r equals one and is *stationary* for $|\psi| = 0$, and then r decreases for increasing values of $|\psi|$. Thus, except for small values of $|\psi|$ for which $r \approx 1$, $r < 1$ and the flux tends to become less oscillating with each freezing-and-thawing cycle. For simplicity, we choose a ψ_c and assume $r = 1$ for $|\psi| < \psi_c$ and $r = 0$ for $|\psi| > \psi_c$ [curve C in Fig. 4(f)]. With the reasonable choice $\psi_c = \pi/5$, this translates into $r = 1$ for $w < w_c$ and $r = 0$ for $w > w_c$, where $w_c = |\csc\theta|/10$ or

$$w_c = \frac{1}{10}\sqrt{1 + \left(\frac{x}{d - b}\right)^2}. \quad (1)$$

For $w > w_c$, $r = 0$ and the beads enter the flowing layer in a thawing flux of constant composition [to see this point, it is helpful to study a case with very high waviness, e.g., Fig. 4(g)], leading to the rapid formation of a *moon* pattern. Thus, a sun pattern of waviness $w > w_c$ is wiped out. On the other hand, for $w < w_c$, $r = 1$ and the beads enter the flowing layer in a thawing flux of oscillating composition [to see this point, it is helpful to study a case with very low waviness, e.g., Fig. 4(h)]. Thus, a sun pattern of waviness $w < w_c$ may persist. We conclude that the waviness of a sun pattern is subjected to low-pass filtering with the cutoff waviness w_c given by (1). The cutoff waviness depends on the fill level, the average composition of the mixture, and the depth of the flowing layer through the variables d, x, and b. The peak value of w_c occurs for $d = b$ (or $d' = 0$). This is consistent with the experiments of Fig. 2(c), in which w peaks for $d = 0.1R$; in fact, we have measured the depth of the flowing layer to be $b \approx 0.1R$ in those experiments.

To test these predictions, we compute $d' = d - b$ (using $b = 0.1R$), d'/x, and w [13] for each of the patterns, transient or steady, that we photographed in the experiments of Fig. 2(c). Then, we plot the point $(w, d'/x)$ for

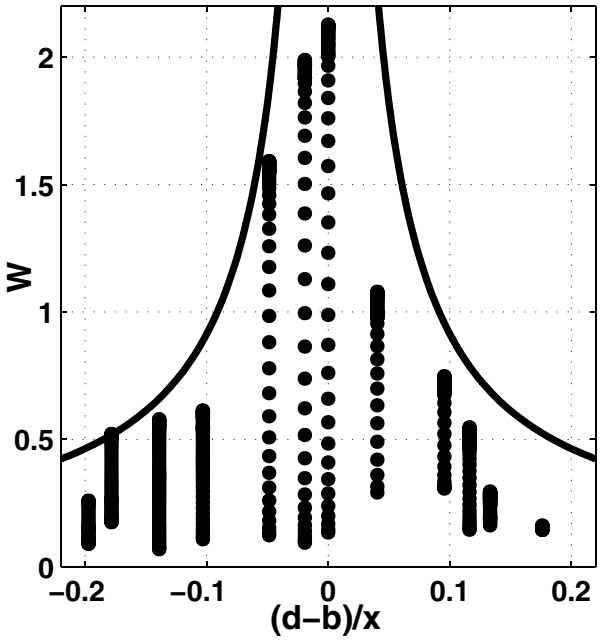

FIG. 5. A comparison of the predictions of the model with the experimental results. The curve represents the predicted cutoff waviness. Each point represents an experimental measurement. Points with the same $(d–b)/x$ correspond to the same experiment; successive points with the same $(d–b)/x$ approach the cutoff waviness as the pattern in the experiment becomes steady.

each pattern (Fig. 5) and the curve w_c vs d'/x predicted by the model. The effect of the low-pass filtering is manifest in Fig. 5: the experimental points lie beneath the theoretical curve. Further, for any given value of d'/x the waviness draws near the cutoff waviness as the pattern becomes steady [14], indicating that the waviness of a steady pattern is *selected* by the low-pass filtering. To understand how this comes about, we turn our attention back to Fig. 2(c), in which a moon pattern has just formed. Now this moon pattern is likely to be slightly wavy; if the drum continues to rotate, the initially low waviness will be amplified [Fig. 2(b)]. (The simulations of Khakhar *et al.* [7] indicate that the amplification takes place *inside* the flowing layer.) By virtue of this amplification, the waviness will increase up to the cutoff value w_c, whereupon the filtering will equilibrate the amplification, bringing the amplification to an end [15]. (Note that for most fill levels w_c is very low, so that the amplification will be arrested shortly after the formation of the moon pattern, which will appear to be steady.)

To summarize: As soon as a moon pattern forms, it is subjected to waviness amplification and low-pass filtering. In time, the filtering arrests the amplification, thereby selecting the waviness of the steady sun pattern. Here we have developed a model of waviness filtering, ignoring the amplification. We have been able to do so because the filtering and the amplification are spatially disjoint: the filtering stems from the way in which the beads move *outside* the flowing layer, whereas the amplification stems from the way in which the beads move *inside* the flowing layer [7]. Thus the filtering depends only on the geometry of the patterns and remains independent of the segregation mechanisms that operate in the flowing layer. On the other hand, the amplification may depend on the difference in bead sizes, the density contrast between the beads and the interstitial fluid, and other factors that pertain to the segregation mechanisms that operate in the flowing layer. We shall take up the development of a model of waviness amplification in a separate paper.

We are grateful for the financial support of the Research Board and the CRI Program at UIUC.

[1] A. Rosato, K. J. Strandburg, F. Prinz, and R. H. Swendsen, Phys. Rev. Lett. **58**, 1038 (1987); J. B. Knight, H. M. Jaeger, and S. R. Nagel, *ibid.* **70**, 3728 (1993); O. Zik, D. Levine, S. G. Shtrikman, and J. Stavans, *ibid.* **73**, 644 (1994); S. B. Savage and C. K. K. Lun, J. Fluid Mech. **189**, 311 (1988); H. A. Makse, S. Havlin, P. R. King, and H. E. Stanley, Nature (London) **386**, 379 (1997).

[2] This might be the first form of granular segregation ever noted in a scientific paper; A. Schoklitsch, Akad. Wiss. **142**, 343 (1933).

[3] The armour layer has often been ascribed to selective erosion [e.g., R. Bettess and A. Frangipane, J. Hydraul. Res. **41**, 179 (2003)], but field data pointing to the importance of granular segregation has been known for a long time [e.g., L. B. Leopold, M. G. Wolman, and J. P. Miller, *Fluvial Processes in Geomorphology* (W. H. Freeman and Co., San Francisco, 1964), Chap. 7].

[4] T. Shinbrot and F. J. Muzzio, Phys. Today **53**, No. 3, 25 (2000).

[5] E. Clement, J. Rajchenbach, and J. Duran, Europhys. Lett. **30**, 7 (1995); F. Cantelaube and D. Bideau, *ibid.* **30**, 133 (1995); D. V. Khakhar, J. J. McCarthy, and J. M. Ottino, Phys. Fluids **9**, 3600 (1997).

[6] K. M. Hill *et al.*, Proc. Natl. Acad. Sci. U.S.A. **96**, 11701 (1999).

[7] D. V. Khakhar, A. V. Orpe, and J. M. Ottino, Powder Technol. **116**, 232 (2001).

[8] If air is the interstitial fluid instead of water, similar patterns form, and the sun patterns occur only in a narrow range of fill levels [6,7], just as in Fig. 2(c). This fact suggests that our analysis could be broadly applicable, in particular, to granular flows in air.

[9] We use NIH Image, which computes the length of the boundary between dark and light areas in a given picture. To calibrate this computation, we use the picture of a moon pattern, for which p can be calculated analytically.

[10] N. Jain, J. M. Ottino, and R. M. Lueptow, Phys. Fluids **14**, 572 (2002); D. Bonamy, F. Daviaud, and L. Laurent, *ibid.* **14**, 1666 (2002); K. M. Hill, G. Gioia, and V. V. Tota, Phys. Rev. Lett. **91**, 064302 (2003).

[11] We take v_n to be constant on the segment Δx of the freezing (or thawing) line.

[12] In our model, a moon pattern becomes wavy when the interface between the black and the white beads, initially a circular arc, becomes undulated with a wavelength λ. Thus the volume of the white stripes is the same as the volume of the black stripes, regardless of the average composition of the mixture.

[13] To estimate w we write $p = 2x + L + 2n\Delta x$, where n is the number of stripes, and $L = (\pi + 2\theta)x\sec\theta$ [Fig. 4(d)]. By substituting $n = 2L/\lambda$ we arrive to the formula $w = (p - 2x - L)/2L$. From the picture of the pattern we obtain p, x, and L, and then estimate w using this formula. For a moon pattern $p = 2x + L$, and $w = 0$.

[14] The case $d'/x = 0$ (which corresponds to $|\psi| = 0$) is an exception, because w_c is singular for $d'/x = 0$. Nevertheless, there exists an upper bound, w_u, on the attainable waviness, and we can *regularize* the cutoff waviness by taking $w_c = w_u$ for $d'/x = 0$. To obtain an expression for w_u, we note that for $d' = 0$ (or $d = b$) the depth of the flowing layer is d, and its half-length R. Thus we can estimate $\Delta x \sim R$ and $\lambda \sim 2b = 2d$, and therefore $w_u \sim R/2d$; for the experiments of Fig. 2(c), $d/R = 0.1$ and we have $w_u \sim 5$, which is in reasonable accord with the peak value of w measured in those experiments (Fig. 5).

[15] We can write an equation of equilibrium between the filtering and the amplification in the form $r_a r = 1$, where $0 < r < 1$ represents the filtering and $r_a > 1$ represents the amplification. For $w = w_c$ (or $\psi = \psi_c$), r can take any value between 0 and 1 [Fig. 4(f)], and the filtering can equilibrate any value of $r_a > 1$.